PHYSICAL REVIEW B VOLUME 57, NUMBER 22 1 JUNE 1998-II

Local voltage-current characteristics in high-T_c superconductors

D. Giller, Y. Abulafia, R. Prozorov, Y. Wolfus, A. Shaulov, and Y. Yeshurun
Institute of Superconductivity, Department of Physics, Bar Ilan University, Ramat Gan, 52900 Israel
(Received 7 January 1998; revised manuscript received 3 March 1998)

Local electric field versus current density (E-j) curves were measured in $YBa_2Cu_3O_{7-\delta}$ and $Nd_{1.85}Ce_{0.15}CuO_{4-\delta}$ single crystals using a miniature Hall-sensors array. Measurements in the field range corresponding to the anomalous magnetization peak in these crystals reveal remarkably different E-j characteristics below and above the peak, indicating a crossover in the flux-creep mechanism. Similar E-j behavior, as observed here in $YBa_2Cu_3O_{7-\delta}$ and $Nd_{1.85}Ce_{0.15}CuO_{4-\delta}$, is expected universally in every superconductor exhibiting the anomalous peak. [S0163-1829(98)50922-8]

Local magnetization measurements, using a linear array of miniature Hall sensors, have emerged as a powerful tool for studying magnetic properties of superconductors.[1–6] Unlike the conventional global techniques in which the total magnetization is recorded, the local technique provides the detailed profile of the magnetic field across the sample. It has been previously shown that the field profile and its time evolution can be effectively utilized in the study of vortex phase transitions[2,3] and vortex dynamics.[4–6] In this paper we describe a new application of this technique in measuring the local electric field vs current density (E-j) curves. Previous magnetic measurements of E vs j,[7] based on global magnetic relaxation data, provide E at the sample surface and the *averaged* j across the sample. In contrast, our local technique enables measurements of E and j at the *same* location. In addition, as discussed below, the local technique enables measurements of E-j curves at a *constant* induction field, a condition which can be hardly achieved in global measurements.

We apply our technique to the study of the flux creep mechanism in $YBa_2Cu_3O_{7-\delta}$ (YBCO) and $Nd_{1.85}Ce_{0.15}CuO_{4-\delta}$ (NCCO) crystals, in the field range corresponding to their anomalous magnetization peak (''fishtail'').[3,5,8,9] The shape and the field range of the fishtail in these crystals is quite different (see Fig. 1). The NCCO crystal ($T_c \approx 23$ K) exhibits a fishtail with a sharp onset at relatively low fields ($H < 500$ G) whereas the YBCO crystal ($T_c \approx 91$ K) exhibits a broad peak at fields of order 1 T. The sharp onset of the peak in NCCO, similar to that observed in $Bi_2Sr_2CaCu_2O_{8+\delta}$ (BSCCO),[10] has been interpreted as signifying a transition from a relatively ordered vortex lattice to a highly disordered entangled solid.[3,11,12] The broad peak in YBCO has been ascribed to either defects[8] or dynamic effects.[9] In this paper we show that despite the qualitative differences between these two systems, both exhibit similar E-j behavior in the field range of the fishtail. In particular, both crystals reveal a crossover in E-j characteristics around the fishtail peak, indicating a crossover in the vortex creep mechanism. As discussed below, such a crossover is expected universally wherever an anomalous magnetization peak is observed.

Flux motion in superconductors creates an electric field **E**, related to the rate of change of the induction **B** through the Maxwell equation $\nabla \times \mathbf{E} = -(1/c)\partial \mathbf{B}/\partial t$. We consider a rectangular sample of a width much smaller than its length (see inset to Fig. 2) and approximate it as an infinite long strip with current flowing parallel to its length along the y axis, $\mathbf{j} = [0, j(x), 0]$. For such a strip in a perpendicular field (parallel to the z axis), $\mathbf{B} = (B_x, 0, B_z)$, $\mathbf{E} = (0, E_y, 0)$, and one obtains

$$\partial E_y / \partial x = -(1/c)\partial B_z / \partial t. \tag{1}$$

Thus,

$$E_y(x,t) = -\frac{1}{c}\int_0^x \frac{\partial B_z(x',t)}{\partial t}\, dx'. \tag{2}$$

In this equation $x = 0$ is the center of the sample where symmetry forces $j = 0$ and $E = 0$. Using the raw $B_z(x,t)$ data we calculate the local relaxation rate $\partial B_z(x,t)/\partial t$ and then spatially integrate it in order to determine the electric field $E(x,t)$ according to Eq. (2). The integration is performed

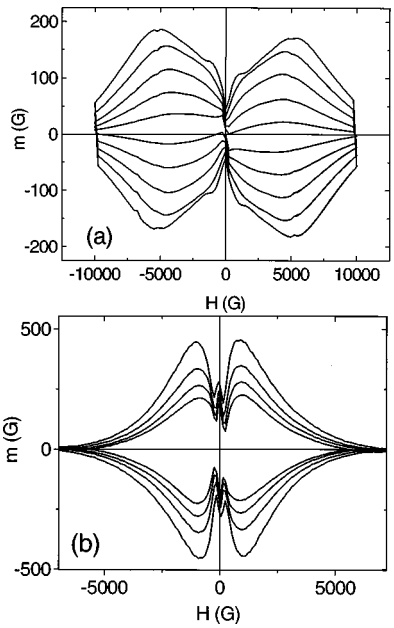

FIG. 1. Local magnetization curves for $YBa_2Cu_3O_{7-\delta}$ and $Nd_{1.85}Ce_{0.15}CuO_{4-\delta}$ crystals at $T = 85$ and 13 K, respectively, exhibiting the anomalous magnetization peak. The width of the loops increases toward the center of the sample.

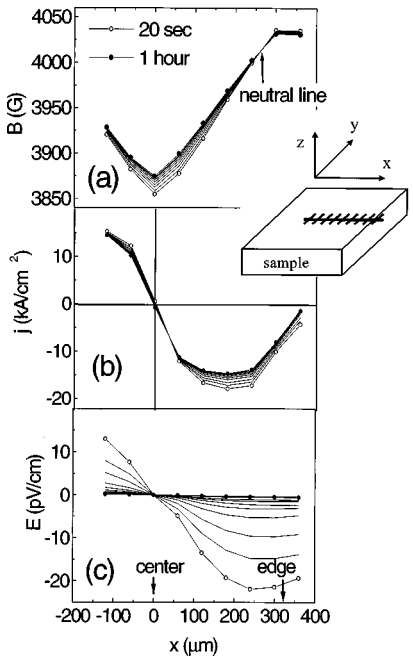

FIG. 2. Typical profiles of (a) $B_z(x,t)$, (b) $j(x,t)$, and (c) $E(x,t)$ at the indicated times for the YBCO crystal, at $T=85$ K and $H=4015$ G. The $B_z(x,t)$ profiles are measured, $j(x,t)$ and $E(x,t)$ are calculated from $B_z(x,t)$ and $\partial B_z/\partial t$, respectively. Lines connecting data points are guides for the eye. Inset: schematic configuration of the Hall sensor array relative to the sample.

numerically using the elementary trapezoidal method. The current distribution $j(x,t)$ across the sample is determined from the same $B_z(x,t)$ data using a one-dimensional inversion scheme. In this approach, the current through the sample is viewed as flowing in N parallel channels, each carrying current of density j_k $(k=1,\ldots,N)$, where N is the total number of the sampling points in the field profile. In N we include all the measured points B_i, and extrapolated points assuming symmetric field profiles with respect to the sample center. The Biot-Savart integral relating $B_z(x,t)$ and $j(x,t)$ is then written in a matrix form: $B_i=M_{ik}j_k$ $(i,k=1,\ldots,N)$, implying that the current density in each channel k contributes to the field B_i. The square matrix M_{ik} can be analytically calculated and inverted to yield the current distribution j_k $(k=1,\ldots,N)$ from the B_i $(i=1,\ldots,N)$ data. For a thorough discussion of the general inversion scheme see Brandt[13] and Wijngaarden.[14]

Measurements of j and E at a certain location during the relaxation process yield the functional dependence of E on j at this location. In general, $E=E(j,B)$, thus it is expected that the $E(j)$ characteristics depend on the location x because of spatial variations of the induction B. Moreover, even at the same location, B varies with time through the relaxation process. In global magnetic measurements it is difficult to overcome these problems and usually the spatial and time dependence of B is overlooked. In contrast, our local measurements offer a simple way to avoid this problem; we determine the E-j curve close to the ''neutral line''[15] where $\partial B_z/\partial t$ is approximately zero, and B_z equals the external magnetic field H. Note that in the presence of an external magnetic field, B_x is usually negligible compared to B_z, thus $B_z \approx B$ and one measures $E(j)$ at a constant B. It should be emphasized that both $j(x,t)$ and $E(x,t)$ are the *average* of the current density and the electric field over the distance between two adjacent Hall sensors. Since both $j(x,t)$ and $E(x,t)$ are expected to vary smoothly across the sample, this averaging process cannot inflict large errors. Obviously, the ''local'' nature and the accuracy of our technique improve as the size of the Hall sensors decreases and their number increases.

Measurements were performed on a $1.20\times0.64\times0.30$ mm^3 YBCO (Ref. 16) and a $1.20\times0.35\times0.02$ mm^3 NCCO (Ref. 17) single crystals having transition temperatures $T_c\approx91$ and 23 K, respectively. An array of microscopic GaAs/AlGaAs Hall sensors, with sensitivity better than 0.1 G, was in direct contact with the surface of the crystal, as shown schematically in the inset to Fig. 2. The active area of each sensor was 30×30 μm^2 for YBCO and 10×10 μm^2 for NCCO. In the experiment, the sample was zero-field cooled from above T_c to the measuring temperature, then a dc magnetic field H was applied parallel to the c axis, and the local induction B_z was subsequently measured at different locations as a function of time for about one hour.

Typical induction profiles $B(x,t)$ at various times are shown in Fig. 2(a) for the YBCO sample at $H=4015$ G and $T=85$ K. The neutral line is indicated by an arrow. Figure 2(a) includes all the data required for the extraction of the current density $j(x,t)$ [from $B_z(x,t)$] and the electric field $E(x,t)$ [from $\partial B_z(x,t)/\partial t$] as explained above. Figures 2(b) and 2(c) show $j(x,t)$ and $E(x,t)$ as deduced from the data of Fig. 2(a). Similar results for $B(x,t)$,$j(x,t)$ and $E(x,t)$ were obtained for the NCCO crystal. Note that according to Eq. (1) the slope of $E(x,t)$ is related to the rate of change of B_z with time. The latter is maximum at the center and drops to zero at the neutral line. The behavior of E is thus consistent with this picture: It has an inflection point at the center and a maximum at the neutral line.[18] Also note that, unlike B_z, both E and j exhibit relaxation at the neutral line as well; the relaxation in E is associated with relaxation in B_z in other locations rather than the neutral line [see Eq. (2)] whereas the relaxation of j is related to relaxation of $\partial B_z/\partial x$ and $\partial B_x/\partial z$ at the neutral line.

From the data shown in Figs. 2(b) and 2(c) one can construct the E-j curves at different locations in the crystal. However, as discussed above, reliable determination of E-j curves at *constant* B is obtained close to the neutral line where B is approximately constant and equals the external field. Figures 3(a) and 3(b) exhibit E-j curves, calculated in this way, for the YBCO and the NCCO crystals, respectively, in the field range corresponding to their anomalous peak effect. In the limited range of the current density all the curves exhibit approximately a power-law dependence, $E\propto j^n$ with an exponent n depending upon the field. Figure 4 shows the power $n=\partial \ln E/\partial \ln j$ as a function of the field for YBCO (circles) and NCCO (squares). In both crystals one clearly sees a dramatic crossover in $n(B)$ near the fish-tail peak. Recalling that $E\propto \exp(-U/kT)$, where U is the activation energy for flux creep, the changes in the exponent n indicate a crossover in the flux creep mechanism. According to the scenario described in Ref. 5, it is a crossover from elastic to plastic creep. This scenario is supported by analysis

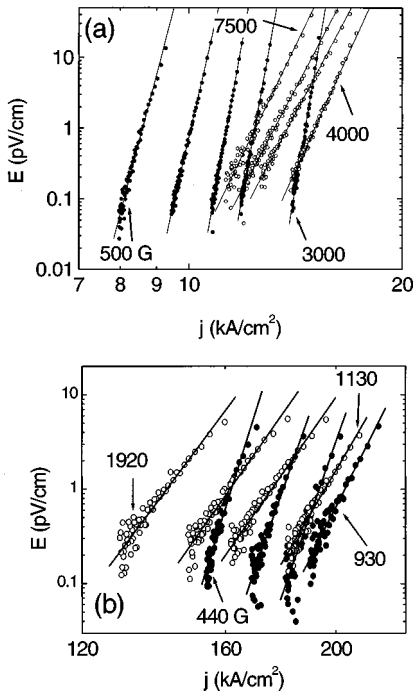

FIG. 3. A log-log plot of the E-j curves, calculated from $j(x,t)$ and $E(x,t)$ close to the neutral line for (a) YBCO and (b) NCCO in the field range corresponding to their anomalous peak effect, measured at $T=85$ and $T=13$ K, respectively. Two typical sets of curves are shown for each crystal, corresponding to fields below and above the peak (full and open circles, respectively). The fields are 500, 1000, 1500, 2000, 3000, 4000, 6000, 6500, and 7500 G for YBCO, and 440, 540, 640, 930, 1130, 1430, 1630, and 1920 G for NCCO. Note the change in the slope above and below the peak field.

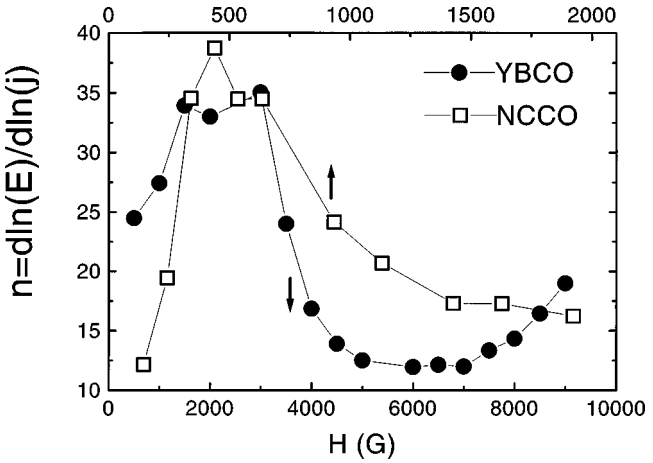

FIG. 4. Field dependence of $n=d\ \ln(E)/d\ \ln(j)$, determined from the data of Fig. 3 for YBCO (circles, lower scale) and NCCO (squares, upper scale).

of the activation energy U which shows that U increases with field below the peak and decreases with field above the peak. While the increase of U with B is consistent with the collective creep theory, the decrease of U cannot be explained in terms of this theory. Nevertheless, a decrease of U with B can be well explained by a dislocation mediated mechanism of plastic creep.[5]

A similar crossover in the flux creep mechanism, and thus in the E-j characteristics, is expected universally in every superconducting material exhibiting the fishtail phenomenon, provided that the persistent current density j is well below the critical current density j_c. One can reach this conclusion considering the behavior of either j vs B, or U vs B. In the first approach, the *increase* of j with B below the fishtail peak is the signature of a collective creep mechanism.[19] However, the *decrease* of j with B above B_p cannot be explained within the collective creep theory,[5,19] unless j is close to j_c.[9] Thus, a crossover to a different flux creep mechanism must take place. In the second approach, considering U vs B, the collective creep activation energy $U_{\rm el}$ increases with field,[19] whereas the activation energy $U_{\rm pl}$ for plastic creep decreases with field.[5] Clearly, the creep process is governed by the smaller between $U_{\rm el}$ and $U_{\rm pl}$. Thus, in the low-field range, where $U_{\rm el}<U_{\rm pl}$, the former controls the flux dynamics. As B increases, at some point $U_{\rm pl}$ becomes less than $U_{\rm el}$, and a crossover to the plastic creep regime takes place.

The arguments of the previous paragraph are general, and can be applied to any superconductor exhibiting a fishtail magnetization, provided that $j \ll j_c$. The condition $j \ll j_c$ is fulfilled for most high-T_c superconductors (HTS) and, in particular, in YBCO (Ref. 5) and NCCO.[3] Thus a universal crossover in the creep mechanism around the fishtail peak is expected, as demonstrated here for YBCO and NCCO, two distinct systems exhibiting different T_c, different anisotropy, and different field range for the fishtail anomaly.

In conclusion, we described a method for measuring the *local* electric-field vs current-density curves from time resolved measurements of the magnetic induction profiles across a superconducting sample. This method allows measurements of the E-j curves in regions hardly accessible by transport measurements. Considering the fact that at the neutral line the induction field is approximately constant, this method allows accurate determination of E-j curves at constant B. The E-j curves in YBCO and NCCO, in the field range of the fishtail, exhibit a crossover in the power-law behavior around the fishtail peak, indicating a crossover in the flux creep mechanism. As argued above, this crossover is expected universally in every HTS exhibiting the fishtail phenomenon.

We thank H. Wühl for providing the $YBa_2Cu_3O_{7-\delta}$ crystal and R. Greene for providing the $Nd_{1.85}Ce_{0.15}CuO_{4-\delta}$ crystal. We acknowledge useful discussions with E. Zeldov and thank H. Shtrikman for growing the GaAs heterostructures. This work was partially supported by the Israel Science Foundations and by the Heinrich Hertz Minerva Center for High Temperature Superconductivity. Y.Y. and A.S. acknowledge support from the German Israeli Foundation (GIF). R.P. acknowledges support from the Clore Foundations.

[1] H. W. Weber, G. P. Westphal, and I. Adaktylos, Cryogenics **16**, 39 (1976); T. Tamegai, L. Krusin-Elbaum, P. Santhanam, M. J. Brady, W. T. Masselink, C. Feild, and F. Holtzberg, Phys. Rev. B **45**, 2589 (1992); M. Konczykowski, L. Burlachkov, Y. Yeshurun, and F. Holtzberg, Physica C **194**, 155 (1992); A. M. Chang, H. D. Hallen, L. Harriot, H. F. Hess, H. L. Kao, J. Kwo, R. E. Miller, R. Wolfe, J. van der Ziel, and T. Y. Chang, Appl. Phys. Lett. **61**, 1974 (1992); T. Tamegai, Y. Iye, I. Oguro, and K. Kishio, Physica C **213**, 33 (1993); D. A. Brawner and N. P. Ong, J. Appl. Phys. **73**, 3890 (1993); S. T. Stoddart, S. J. Bending, A. K. Geim, and M. Henini, Phys. Rev. Lett. **71**, 3854 (1993); A. Oral, S. J. Bending, and M. Henini, Appl. Phys. Lett. **61**, 1974 (1996).

[2] E. Zeldov, A. I. Larkin, V. B. Geshkenbein, M. Konczykowski, D. Majer, B. Khaykovich, V. M. Vinokur, and H. Shtrikman, Phys. Rev. Lett. **73**, 1428 (1994); E. Zeldov, D. Majer, M. Konczykowski, V. B. Geshkenbein, V. M. Vinokur, and H. Shtrikman, Nature (London) **375**, 373 (1995); B. Khaykovich, E. Zeldov, D. Majer, T. W. Li, P. H. Kes, and M. Konczykowski, Phys. Rev. Lett. **76**, 2555 (1996); B. Khaykovich, M. Konczykowski, E. Zeldov, R. Doyle, D. Majer, P. H. Kes, and T. W. Li, Phys. Rev. B **56**, R517 (1997).

[3] D. Giller, A. Shaulov, R. Prozorov, Y. Abulafia, Y. Wolfus, L. Burlachkov, Y. Yeshurun, E. Zeldov, V. M. Vinokur, J. L. Peng, and R. L. Greene, Phys. Rev. Lett. **79**, 2542 (1997).

[4] Y. Abulafia, A. Shaulov, Y. Wolfus, R. Prozorov, L. Burlachkov, Y. Yeshurun, D. Majer, E. Zeldov, and V. M. Vinokur, Phys. Rev. Lett. **75**, 2404 (1995).

[5] Y. Abulafia, A. Shaulov, Y. Wolfus, R. Prozorov, L. Burlachkov, Y. Yeshurun, D. Majer, E. Zeldov, H. Wuhl, V. B. Geshkenbein, and V. M. Vinokur, Phys. Rev. Lett. **77**, 1596 (1996).

[6] Y. Abulafia, D. Giller, Y. Wolfus, A. Shaulov, Y. Yeshurun, D. Majer, E. Zeldov, J. L. Peng, and R. L. Greene, J. Appl. Phys. **81**, 4944 (1997).

[7] E. Sandvold and C. Rossel, Physica C **190**, 309 (1992); M. Konczykowski, V. Vinokur, F. Rullier-Albenque, Y. Yeshurun, and F. Holtzberg, Phys. Rev. B **47**, R5531 (1993); H. Küpfer, S. N. Gordeev, W. Jahn, R. Kresse, R. Meier-Hirmer, T. Wolf, A. A. Zhukov, K. Salama, and D. Lee, *ibid.* **50**, 7016 (1994); for a recent review see Y. Yeshurun, M. P. Malozemoff, and A. Shaulov, Rev. Mod. Phys. **68**, 911 (1996).

[8] M. Daeumling, J. M. Seutjens, and D. C. Larbalestier, Nature (London) **346**, 332 (1990); L. Klein, E. R. Yacoby, Y. Yeshurun, A. Erb, G. Muller-Vogt, V. Breit, and H. Wuhl, Phys. Rev. B **49**, 4403 (1994).

[9] L. Krusin-Elbaum, L. Civale, V. M. Vinokur, and F. Holtzberg, Phys. Rev. Lett. **69**, 2280 (1992); Y. Yeshurun, E. R. Yacoby, L. Klein, L. Burlachkov, R. Prozorov, N. Bontemps, H. Wuhl, and V. Vinokur, in *Critical Currents in Superconductors*, Proceedings of the 7th IWCC, Austria, edited by H. W. Weber (World Scientific, Singapore, 1994), pp. 237–239.

[10] Y. Yeshurun, N. Bontemps, L. Burlachkov, and A. Kapitulnik, Phys. Rev. B **49**, 1548 (1994); D. Majer, E. Zeldov, H. Shtrikman, and M. Konczykowski, in *Coherence in High-T_c Superconductors*, edited by A. Revolevschi and G. Deutscher (World Science, Singapore, 1996), p. 271.

[11] D. Ertas and D. R. Nelson, Physica C **272**, 79 (1996).

[12] V. Vinokur, B. Khaykovich, E. Zeldov, M. Konczykowski, R. A. Doyle, and P. Kes, Physica C **295**, 209 (1998).

[13] E. H. Brandt, Phys. Rev. Lett. **74**, 3025 (1995).

[14] R. J. Wijngaarden, H. J. W. Spoelder, R. Surdeanu, and R. Griessen, Phys. Rev. B **54**, 6742 (1996).

[15] The neutral line is the contour of points in the sample for which the z component of the induction field equals the external field H. For a platelet sample in a perpendicular field, the sample contribution to the induction field **B** is composed of components parallel (B_z) and perpendicular (B_x) to the applied field. As a result of demagnetization, the sample contribution to B_z has a different sign at the edge and the center, and there exists a contour inside the sample where $B_z = H$ exactly. The neutral line has been observed in magneto-optic measurements by T. Schuster, H. Kuhn, and E. H. Brandt, Phys. Rev. B **51**, 697 (1995); as well as in Hall array measurements by Y. Abulafia, A. Shaulov, Y. Wolfus, R. Prozorov, L. Burlachkov, D. Majer, E. Zeldov, V. Vinokur, and Y. Yeshurun, Low Temp. Phys. **107**, 455 (1996).

[16] A. Erb, T. Traulsen, and G. Muller-Vogt, J. Cryst. Growth **137**, 487 (1994).

[17] J. L. Peng, Z. Y. Li, and R. L. Greene, Physica C **177**, 79 (1991).

[18] E. H. Brandt, Phys. Rev. B **52**, 15 442 (1995).

[19] G. Blatter, M. V. Feigel'man, V. B. Geshkenbein, A. I. Larkin, and V. M. Vinokur, Rev. Mod. Phys. **66**, 1125 (1994).